Supporting Information

Ni_3N/NF as bifunctional catalysts for both hydrogen generation and urea decomposition

Shengnan Hu[a], Chuanqi Feng[a], Shiquan Wang[a], Jianwen Liu[a], Huimin Wu[a,*], Lei Zhang[b,c], Jiujun Zhang[b,*]

[a] Hubei Collaborative Innovation Center for Advanced Organic Chemical Materials & Key Laboratory for the Synthesis and Application of Organic Functional Molecules, Ministry of Education & College of Chemistry & Chemical Engineering, Hubei University, Wuhan 430062, PR China

[b] Institute for Sustainable Energy/College of Sciences, Shanghai University, Shanghai, 200444 China

[c] Energy, Mining & Environment, National Research Council of Canada, Vancouver, BC, V6T 1W5, Canada

* Corresponding author. Tel.: 86 27 88662747; Fax: 86 27 88663043.

E-mail address: whm267@hubu.edu.cn; jiujun.zhang@i.shu.edu.cn

Table of contents

Ⅰ XRD patterns of Ni_3N/NF, $Ni(OH)_2$/NF, Ni/NF

Figure S1 shows the XRD patterns of $Ni(OH)_2$/NF, Ni/NF, Obviously, the diffraction peaks at 33.1°, 59.1° and 72.7° are indexed to the (100), (110) and (201) of $Ni(OH)_2$ (JCPDS No. 14-0117). The peaks at 44.5°, 51.8°, 76.6° are belonged to (111), (200), (100) of Ni (JCPDS No. 04-0850), which are from NF.

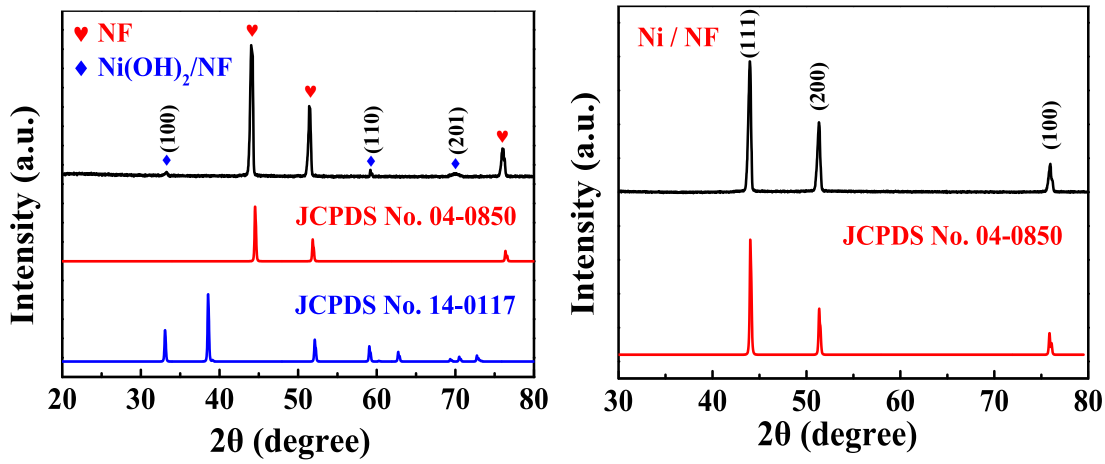

Figure S1. XRD patterns of $Ni(OH)_2$/NF, Ni/NF.

Ⅱ SEM images of bare Ni foam, Ni_3N/NF, $Ni(OH)_2$/NF, Ni/NF

Figure S2(a) displays the SEM image of bare NF, indicating the surface is smooth. The SEM images of $Ni(OH)_2$/NF (**Figure S2(b)**) reveals the gracile nanowire arrays grow uniformly on NF. **Figure S2(c)** showed the SEM image of Ni/NF, it is clearly the distribution of Ni is fluffy and flexible. **Figure S2(d)** reflects the SEM image of the Ni_3N/NF. We can see that the entire surface of NF is evenly covered by Ni_3N.

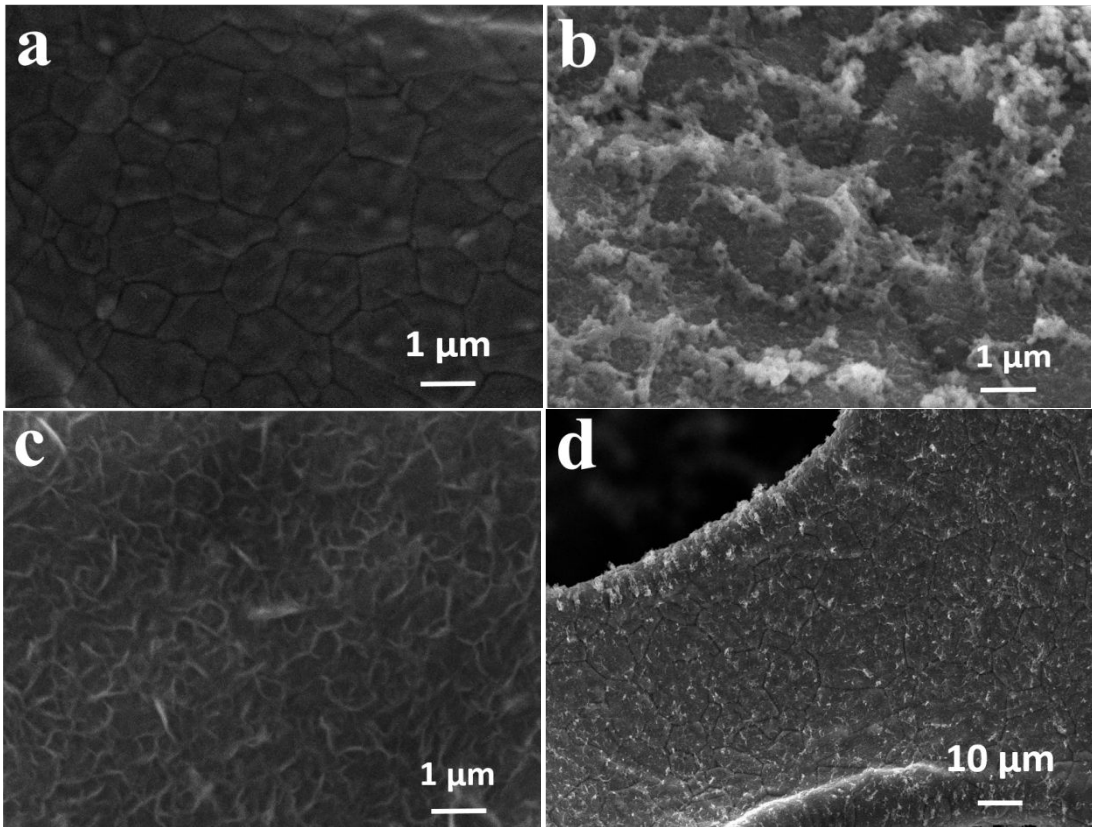

Figure S2. (a) SEM image of bare Ni foam. (b) SEM image of Ni/NF. (c) SEM images of $Ni(OH)_2$/NF. (d) SEM images of Ni_3N/NF.

Ⅲ LSV curves of Ni_3N/NF in 1.0 M KOH with different urea concentration

In order to optimize catalytic performance of UOR, we conducted the LSV of Ni3N/NF in 1.0 M KOH with different urea concentration (from 0.1 to 0.6 M urea). Obviously, the potential of Ni_3N/NF is the lowest in 1.0 M KOH containing 0.5 M urea at the same current density. Therefore, the urea concentration of 0.5 M was chosen for the electrochemical test of UOR.

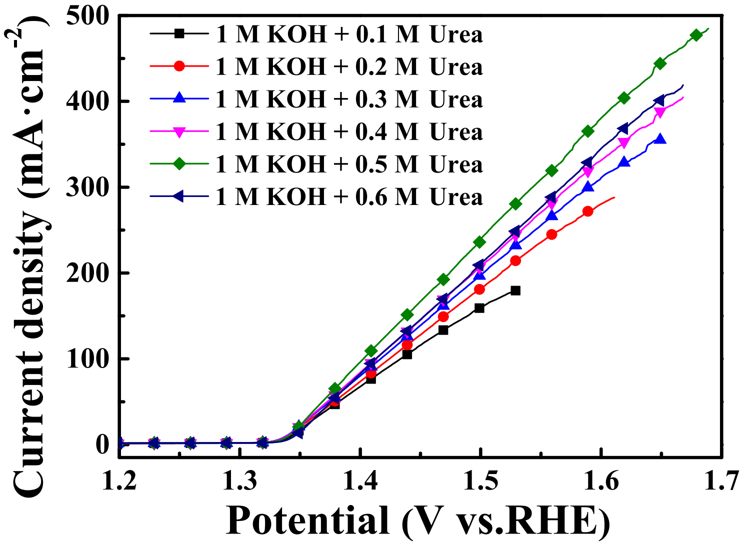

Figure S3. LSV curves of Ni_3N/NF in 1.0 M KOH with 0.1, 0.2, 0.3, 0.4, 0.5 and 0.6 M urea, respectively.

Ⅳ Nyquist plots of Ni_3N/NF, $Ni(OH)_2$/NF, Ni/NF, bare NF and IrO_2

Figure S4(a) shows Nyquist plots of Ni_3N/NF in different electrolytes. Apparently, the conductivity of 1 M KOH with 0.5 M urea is better than 1 M KOH and 0.5 M urea. This implies Ni_3N/NF have faster electron transfer rate in 1 M KOH with 0.5 M urea. Furthermore, the conductivity of the prepared materials was measured. **Figure S4(b)** indicates the R_{ct} of Ni_3N/NF, $Ni(OH)_2$/NF, Ni/NF, bare NF and IrO_2 are corresponded to 2.85 Ω, 8.2 Ω, 8.85 Ω, 9.29 Ω and 4.84 Ω. Obviously, the R_{ct} of nanophere Ni_3N/NF is the lowest. So, Ni_3N/NF has faster electron transfer rate than other prepared catalysts.

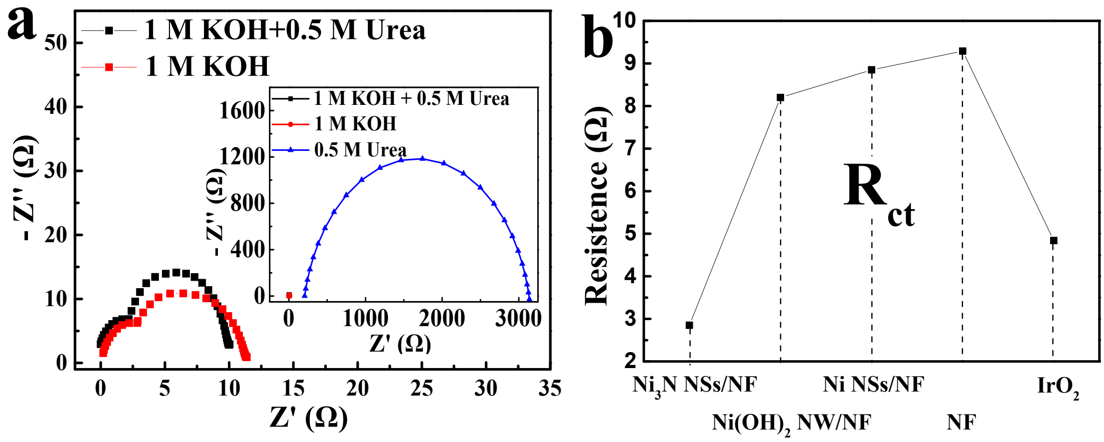

Figure S4. (a) Nyquist plots of Ni_3N/NF in different electrolyte. (b) R_{ct} of Ni_3N/NF, $Ni(OH)_2$/NF, Ni/NF, bare NF and IrO_2.

Ⅴ XRD pattern and XPS spectra of Ni_3N/NF after 3000 cycles

Figure S5(a) and **Figure S5(a*)** shows XRD pattern of Ni_3N/NF after 3000 cycles in HER and UOR, respectively. Obviously, the peaks are almost the same as those before 3000 cycles, matches well with the standard cards. Meanwhile, XPS spectras of Ni 2p, and N 1s for Ni_3N/NF after 3000 cycles are almost the same as those before 3000 cycles (**Figure S5(b, c)** and **Figure S5(b*, c*)**). SEM images of Ni_3N/NF after 3000 cycles in HER and UOR, respectively also maintain the same appearance as before 3000 cycles (**Figure S5(d)** and **Figure S5(d*)**). These results indicate Ni_3N/NF has an excellent stability.

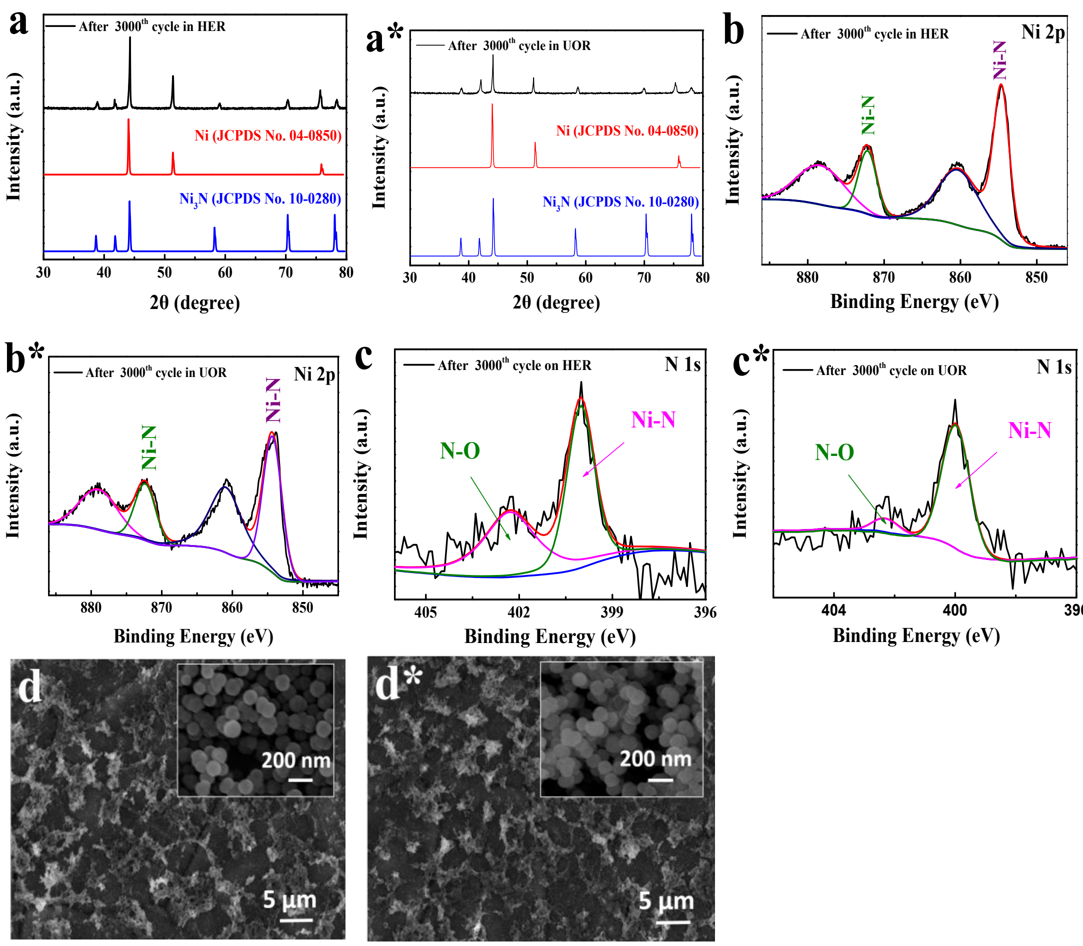

Figure S5. (a) XRD pattern, (b, c) XPS spectras and (d) SEM image of Ni_3N/NF after 3000 cycles in HER. (a*) XRD pattern, (b*, c*) XPS spectras and (d*) SEM image of Ni_3N/NF after 3000 cycles in UOR.

Ⅵ STEM-EDX mapping images of Ni_3N/NF

Figure S6 shows the STEM-EDX mapping images of Ni_3N/NF. We found that the N elements are evenly distributed, while the nickel elements are more densely. It implies Ni_3N is grown on nickel foam.

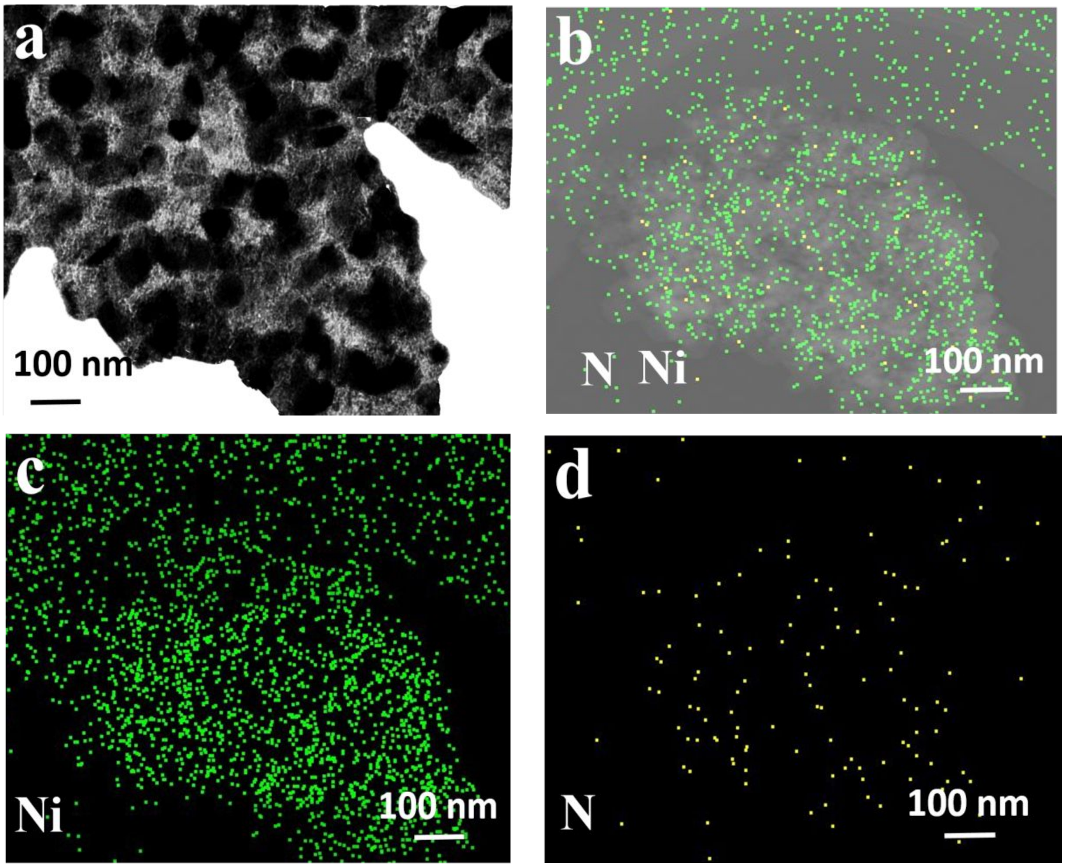

Figure S6. (a) STEM-EDX mapping images of Ni_3N/NF. (b) element mapping of combinations of Ni and N. (c) element mapping of Ni. (d) element mapping of N.

Ⅻ CV curves of Ni_3N/NF, $Ni(OH)_2$/NF, Ni/NF

Figure S7 shows CV curves of Ni_3N/NF, $Ni(OH)_2$/NF, Ni/NF, respectively, in the non-faradic potential region (1.007 V to 1.147 V) at different scan rates (from 5 to 50 mV·s^{-1}). **Figure S7(d)** and **Figure S7(f)** indicate the C_{dl} at 1.077 V is 4.5 and 2.3 mF·cm^{-2} for $Ni(OH)_2$/NF and Ni/NF, respectively. They are all lower than that of Ni_3N/NF (6.45 mF·cm^{-2}) (**Figure S7(b)**). The results show the surface roughness of Ni_3N/NF is higher than the precursors.

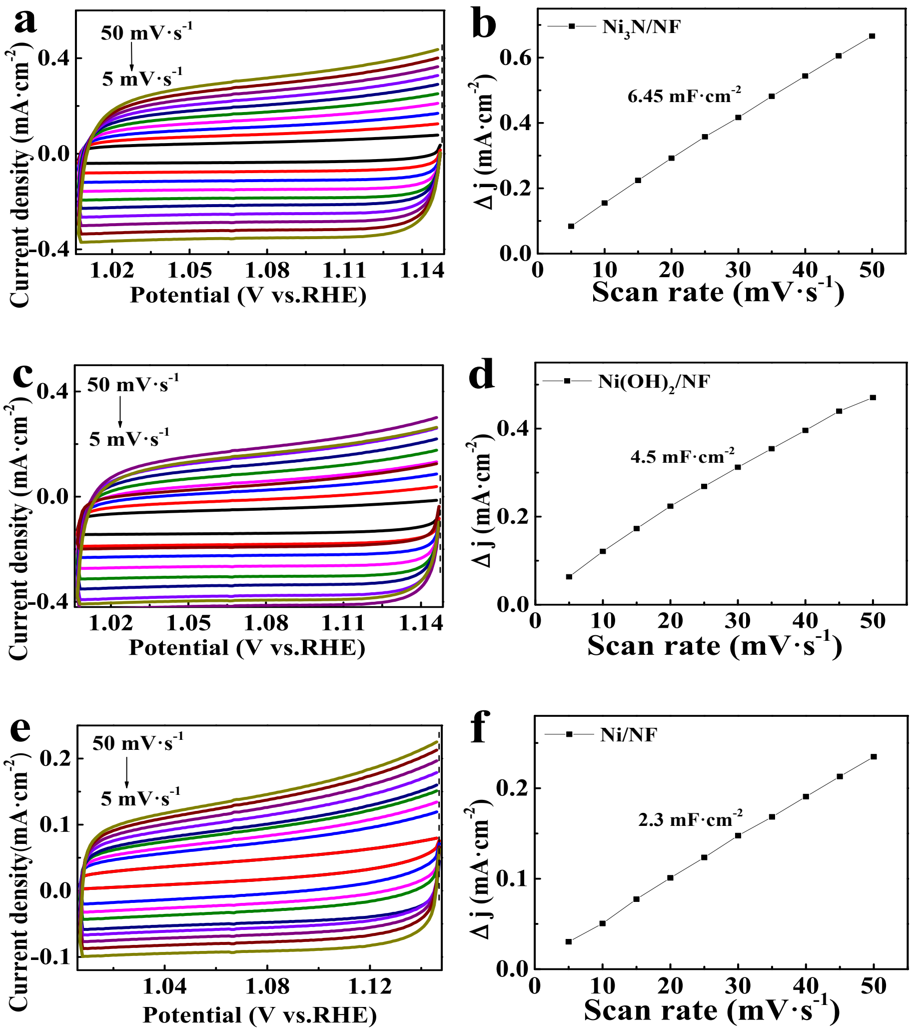

Figure S7. (a), (c) and (e) CV curves of Ni_3N/NF, $Ni(OH)_2$/NF, Ni/NF, respectively, at different scan rates. (b), (d) and (f) C_{dl} for Ni_3N/NF, $Ni(OH)_2$/NF, Ni/NF, respectively.

Ⅷ Comparison of electrochemical performance of Ni_3N/CC cell in the literature

So far, only one used nickel nitride for urea electrolysis.[1] The nickel nitride on carbon cloth was synthesized (Ni_3N/CC) in that literature and its electrochemical performance has been compared. Obviously, the cell voltages of Ni_3N/NF cell we prepared is much lower to that of Ni_3N/CC cell. It implies the catalytic activity of Ni_3N/NF cell is far superior to that of Ni_3N/CC cell.

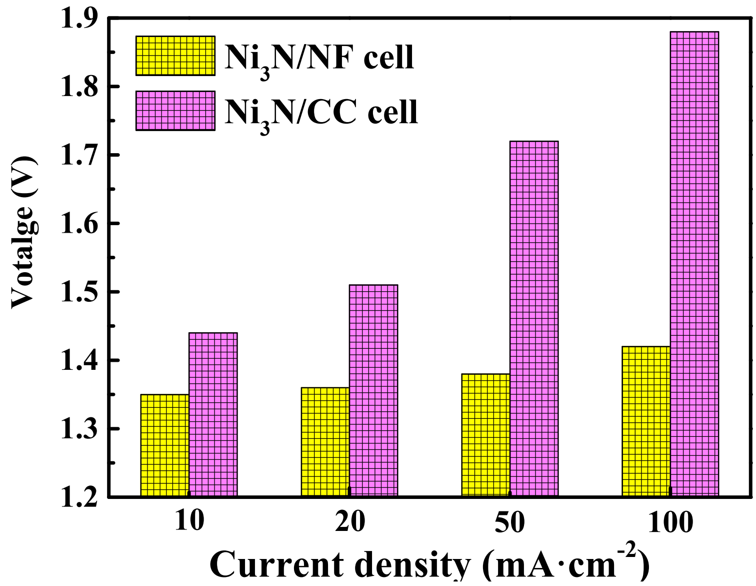

Figure S8. Histogram of Ni_3N/NF and Ni_3N/CC.

Ⅳ Comparison of catalytic performance of some UOR catalysts in recent years

Comparing the catalytic performance of catalysts for UOR in recent years. Obviously, we can discover that the potential of the materials we prepared are lower than that of the most of UOR catalysts. This implies Ni_3N/NF has superior catalytic activity and greater commercial possibilities.

Table S1. Comparison of the UOR activity for several recently reported catalysts.

Catalyst	Potential at 10 $mA\cdot cm^{-2}$(V vs· RHE)	Mass loading($mg\cdot cm^{-2}$)	Reference
Ni_3N/NF	**1.34**	**0.075**	**This work**
Ni_3N NA/CC	**1.35**	**1.9**	**1**
Ni_2P/NF	**1.37**	**0.92**	**2**
$Ni(OH)_2$ nanotube-NF	**1.41**	**-**	**3**
NiO nanosheet array	**1.38**	**0.27**	**4**
ERGO-Ni	**1.45**	**-**	**5**
Graphene $Ni(OH)_2$	**1.52**	**0.25**	
NiCo alloy	**1.53**	**10**	**6**
NiMo sheet array	**1.37**	**0.75**	**7**
L-MnO_2	**1.37**	**1.5**	**8**
$Ni(OH)_2$ nanocube	**1.55**	**0.3**	**9**
Rhodium-Ni	**1.47**	**0.7**	**10**
Nickel film	**1.48**	**1.3**	**11**
Nickel nanowire	**1.44**	**1.3**	
Ni foil	**1.40**	**2**	**12**
Rh-Ni	**1.44**	**2**	

Ⅹ Comparison of the performance of as-prepared catalysts in this work

Comparing the performance of the catalysts prepared in this paper. It is clear that the performance of Ni3N/NF has exceeded Pt/C. This means it has a high probability of becoming a substitute for precious metals.

Table S2. Comparison of the performance of the catalysts in this study

		Ni_3N/NF		
	10mA·cm^{-2}	**100mA·cm^{-2}**	**200mA·cm^{-2}**	**Tafel slope/ mV·dec^{-1}**
UOR(vs· RHE)	**1.340V**	**1.403V**	**1.476V**	**41**
OER(vs· RHE)	**1.580V**	**1.760V**	**/**	**102**
HER(vs· RHE)	**120mV**	**243mV**	**335mV**	**110**
		$Ni(OH)_2/NF$		
UOR(vs· RHE)	**1.352V**	**1.43V**	**1.516V**	**50**
HER(vs· RHE)	**138mV**	**336mV**	**/**	**180**
		Ni/NF		
UOR(vs· RHE)	**1.359V**	**1.482V**	**1.597V**	**58**
HER(vs· RHE)	**211mV**	**371mV**	**/**	**145**

References

(1) Liu, Q.; Xie, L.; Qu, F.; Liu, Z.; Du, G.; Asiri, A. M.; Sun, X. Porous Ni_3N Nanosheets Array as a High-Performance Nonnoble-Metal Catalyst for Urea-Assisted Electrochemical Hydrogen Production. *Inorg. Chem. Front.* **2017**, *4*, 1120-1124.

(2) Liu, D.; Liu, T.; Zhang, L.; Qu, F.; Asiri, A.; Sun, X. High-Performance Urea Electrolysis Towards Less Energy-Intensive Electrochemical Hydrogen Production Using a Bifunctional Catalyst Electrode. *J. Mater. Chem. A* **2017**, *5*, 3208-3213.

(3) Ji, R.; Chan, D.; Jow, J.; Wu, M. Formation of Open-Ended Nickel Hydroxide Nanotubes on Three-Dimensional Nickel Framework for Enhanced Urea Electrolysis, *Electrochem. Commun.* **2013**, *29*, 21-24.

(4) Wu, M.; Lin, G.; Yang, R. Hydrothermal Growth of Vertically-Aligned Ordered Mesoporous Nickel Oxide Nanosheets on Three-Dimensional Nickel Framework for Electrocatalytic Oxidation of Urea in Alkaline Medium. *J. Power Sources* **2014**, *272*, 711-718.

(5) Wang, D.; Yan, W.; Vijapur, S.; Bottte, G. Electrochemically Reduced Graphene Oxide–Nickel Nanocomposites for Urea Electrolysis. *Electrochim. Acta* **2013**, *89*, 732-736.

(6) Xu, W.; Zhang, H.; Li, G.; Wu, Z. Nickel-Cobalt Bimetallic Anode Catalysts for Direct Urea Fuel Cell. *Sci. Rep.* **2014**, *4*, 58-63.

(7) Liang, Y.; Lin, Q.; Asiri, A.; Sun, X. Enhanced Electrooxidation of Urea Using NiMoO4 • xH_2O Nanosheet Arrays on Ni Foam as Anode. *Electrochim. Acta* **2015**, *153*, 456-460.

(8) Chen, S.; Duan, J.; Vasileff, A.; Qiao, S. Size Fractionation of Two-Dimensional Sub-Nanometer Thin Manganese Dioxide Crystals towards Superior Urea Electrocatalytic Conversion. *Angew. Chem. Int. Ed.* **2016**, *128*, 3868-3872.

(9) Wu, M.; Ji, R.; Zheng, Y. Nickel Hydroxide Electrode with a Monolayer of Nanocup Arrays as an Effective Electrocatalyst for Enhanced Electrolysis of Urea. *Electrochim. Acta* **2014**, *144*, 194-199.

(10) Miller, A.; Hassler, B.; Botte, G. Rhodium Electrodeposition on Nickel Electrodes Used for Urea Electrolysis. *J. Appl. Electrochem.* **2012**, *42*, 925-934.

(11) Yan, W.; Wang, D.; Diaz, L.; Botte, G. Nickel Nanowires as Effective Catalysts for Urea Electro-Oxidation. *Electrochim. Acta* **2014**, *134*, 266-271.

(12) King, R.; Botte, G. Investigation of Multi-Metal Catalysts for Stable Hydrogen Production Via Urea Electrolysis. *J. Power Sources* **2011**, *196*, 9579-9584.